ORGANIC LETTERS

2013
Vol. 15, No. 14
3582–3585

Ratiometric Fluorescent Probes for Detection of Intracellular Singlet Oxygen

Dayoung Song,[†] Somin Cho,[†] Yejee Han,[†] Youngmin You,*[,‡] and Wonwoo Nam*[,†]

Department of Bioinspired Science, Ewha Womans University, Seoul 120-750, Korea, and Department of Advanced Materials Engineering for Information and Electronics, Kyung Hee University, Yongin-si, Gyeonggi-do 446-701, Korea

odds2@khu.ac.kr (YY); wwnam@ewha.ac.kr (WN)

Received May 20, 2013

ABSTRACT

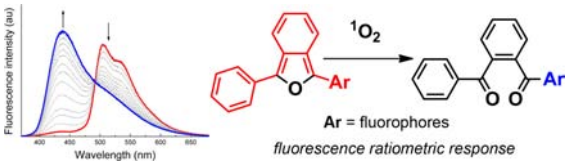

We have developed a series of molecular probes for the fluorescent detection of singlet dioxygen ($^1O_2$). The probes, based on asymmetrically substituted 1,3-diarylisobenzofurans, undergo the [2 + 4] cycloaddition reaction with $^1O_2$, producing ratiometric fluorescent responses. Two-photon fluorescence microscope experiments demonstrated the biological utility of the probes for the visualization of endogenous $^1O_2$ in macrophage cells.

Singlet dioxygen ($^1O_2$) is a highly reactive oxygen species (hROS) that oxidizes a broad range of biomolecules, such as nucleic acids,[1−3] lipids,[4] and proteins.[4−6] These $^1O_2$ oxidation chemistries provide key mechanisms in the regulation of intracellular signaling pathways[7−11] and thus are critically linked to human pathophysiology. However, studies toward understanding molecular mechanisms of $^1O_2$ in vivo have been significantly retarded by difficulties due to its short half-life ($\tau_{1/2}$ = 10^{-6} to 10^{-5} s) in the aqueous milieu.[12] Furthermore, direct monitoring of the phosphorescence of $^1O_2$ lacks practical utility because the emission features very low photoluminescence quantum yields (PLQYs ≈ 10^{-6}).[13] Thus there is a strong need for $^1O_2$ probes with high sensitivity and large dynamic ranges.

Among various probes, photoluminescent probes are the most attractive because they provide many advantages in bioimaging applications.[14] Fluorescent $^1O_2$ probes have been developed by conjugating $^1O_2$ traps and fluorophores, such as fluorescein,[15−17] poly(fluorene),[18−20] cyanine,[21] a Eu(III) complex,[22] and a Re(I) complex.[23] Reactive dienes, including 9,10-disubstituted anthracene[15−18,20,22,23] and

[†] Ewha Womans University.
[‡] Kyung Hee University.

(1) Kang, P.; Foote, C. S. *J. Am. Chem. Soc.* **2002**, *124*, 4865–4873.
(2) Cadet, J.; Bellon, S.; Berger, M.; Bourdat, A.-G.; Douki, T.; Duarte, V.; Frelon, S.; Gasparutto, D.; Muller, E.; Ravanat, J.-L.; Sauvaigo, S. *Biol. Chem.* **2002**, *383*, 933–943.
(3) Ravanat, J.-L.; Cadet, J. *Chem. Res. Toxicol.* **1995**, *8*, 379–388.
(4) Wilkinson, F.; Helman, W. P.; Ross, A. B. *J. Phys. Chem. Ref. Data* **1995**, *24*, 663–1021.
(5) Davies, M. J. *Biochem. Biophys. Res. Commun.* **2003**, *305*, 761–770.
(6) Matheson, I. B. C.; Etheridge, R. D.; Kratowich, N. R.; Lee, J. *Photochem. Photobiol.* **1975**, *21*, 165–171.
(7) Klotz, L.-O.; Kröncke, K.-D.; Sies, H. *Photochem. Photobiol. Sci.* **2003**, *2*, 88–94.
(8) Ryter, S. W.; Tyrrell, R. M. *Free Radical Biol. Med.* **1998**, *24*, 1520–1534.
(9) Wang, X.; Martindale, J. L.; Liu, Y.; Holbrook, N. J. *Biochem. J.* **1998**, *333*, 291–300.
(10) Kröncke, K.-D.; Klotz, L.-O.; Suschek, C. V.; Sies, H. *J. Biol. Chem.* **2002**, *277*, 13294–13301.
(11) Klotz, L.-O.; Briviba, K.; Sies, H. *Methods Enzymol.* **2000**, *319*, 130–143.
(12) Lindig, B. A.; Rodgers, M. A. J. *J. Phys. Chem.* **1979**, *83*, 1683–1688.
(13) Schweitzer, C.; Schmidt, R. *Chem. Rev.* **2003**, *103*, 1685–1757.
(14) Gomes, A.; Fernandes, E.; Lima, J. L. F. C. *J. Biochem. Biophys. Methods* **2005**, *65*, 45–80.
(15) Umezawa, N.; Tanaka, K.; Urano, Y.; Kikuchi, K.; Higuchi, T.; Nagano, T. *Angew. Chem., Int. Ed.* **1999**, *38*, 2899–2901.
(16) Tanaka, K.; Miura, T.; Umezawa, N.; Urano, Y.; Kikuchi, K.; Higuchi, T.; Nagano, T. *J. Am. Chem. Soc.* **2001**, *123*, 2530–2536.
(17) Gollmer, A.; Arnbjerg, J.; Blaikie, F. H.; Pedersen, B. W.; Breitenbach, T.; Daasbjerg, K.; Glasius, M.; Ogilby, P. R. *Photochem. Photobiol.* **2011**, *87*, 671–679.
(18) Koylu, D.; Sarrafpour, S.; Zhang, J.; Ramjattan, S.; Panzer, M. J.; Thomas, S. W., III *Chem. Commun.* **2012**, *48*, 9489–9491.
(19) Altınok, E.; Friedle, S.; Thomas, S. W., III *Macromolecules* **2013**, *46*, 756–762.
(20) Zhang, J.; Sarrafpour, S.; Pawle, R. H.; Thomas, S. W., III *Chem. Commun.* **2011**, *47*, 3445–3447.
(21) Xu, K.; Wang, L.; Qiang, M.; Wang, L.; Li, P.; Tang, B. *Chem. Commun.* **2011**, *47*, 7386–7388.
(22) Song, B.; Wang, G.; Tan, M.; Yuan, J. *J. Am. Chem. Soc.* **2006**, *128*, 13442–13450.
(23) Liu, Y.-J.; Wang, K.-Z. *Eur. J. Inorg. Chem.* **2008**, 5214–5219.

10.1021/ol401421r
Published on Web 06/28/2013

histidine,[21] served as the $^1O_2$ traps, and fluorescence responses were obtained after the [2 + 4] cycloaddition reactions between $^1O_2$ and the traps. The utility of these probes has been limited because their monotonic fluorescence turn-on or turn-off responses suffer from artifacts associated with sensor localization and instrumental drifts.[15−17,19,21−23] In addition, some fluorophores, such as chlorinated fluorescein, convert ground-state dioxygen ($^3O_2$) into $^1O_2$ under photoexcitation,[17,24] which would severely alter the cellular $^1O_2$ levels. Furthermore, probes examined for their utility for the detection of biological $^1O_2$ are extremely rare.[21,22] These drawbacks present a strong rationale for development of new probes capable of ratiometric fluorescent detection and minimized $^1O_2$ photosensitization.

1,3-Diphenylisobenzofuran (DPBF) is an attractive platform for the construction of $^1O_2$ probes because it rapidly reacts with $^1O_2$ at a rate constant of $9.6 \times 10^8\ M^{-1}\ s^{-1}$ in water[25,26] and because it does not photosensitize $^1O_2$ due to effective suppression of the triplet state population.[27] However, the $^1O_2$ products, an endoperoxide or 1,2-dibenzoylbenzene, are nonfluorescent. Thus DPBF itself offers little practical utility for $^1O_2$ detection. We envisioned that the

Scheme 1. Ratiometric Fluorescent Probes for Detection of $^1O_2$

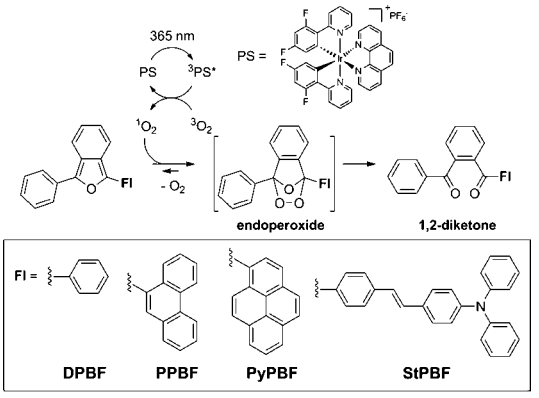

displacement of the phenyl moiety of DPBF with fluorescent chromophores will produce ratiometric fluorescent $^1O_2$ responses: the π-conjugation over 1-phenylisobenzofuran and the chromophore would be shortened by the $^1O_2$ reaction to give hypsochromically shifted fluorescence emission instead of fluorescence turn-off (see Scheme 1). To test this idea, we designed a series of $^1O_2$ probes comprising phenanthrene (PPBF), pyrene (PyPBF), and 4-(diphenylamino)stilbene (StPBF) as fluorophores. Herein, we report the design, syntheses, sensing properties, and biological applications of the novel ratiometric fluorescent $^1O_2$ probes. Fluorescent responses of the probes were compared to correlate $^1O_2$ sensitivity and the extent of π-conjugation.

(24) Gandin, E.; Lion, Y.; Vorst, A. V. d. *Photochem. Photobiol.* **1983**, *37*, 271–278.
(25) Onitsuka, S.; Nishino, H.; Kurosawa, K. *Tetrahedron* **2001**, *57*, 6003–6009.
(26) Aubry, J.-M.; Pierlot, C.; Rigaudy, J.; Schmidt, R. *Acc. Chem. Res.* **2003**, *36*, 668–675.
(27) Zhang, X.-F.; Li, X. *J. Lumin.* **2011**, *131*, 2263–2266.

Scheme 2. Synthesis of StPBF, a Ratiometric Fluorescent Probe for $^1O_2$[a]

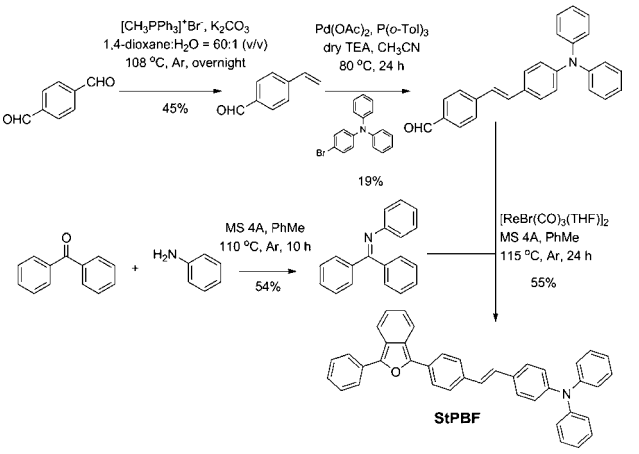

[a] The synthetic routes to other probes are shown in the Supporting Information.

Synthetic routes to StPBF are depicted in Scheme 2. The syntheses of PPBF and PyPBF are described in the Supporting Information (Scheme S1). The fluorophore, a 4-(diphenylamino)stilbene unit, was obtained through the two-step synthesis, comprising a Horner−Wadsworth−Emmons olefination followed by a Pd(II)-catalyzed Heck reaction. The Re(I) dimer catalysis protocol established by the group of Kuninobu and Takai was employed for the construction of the isobenzofuran unit.[28] The $^1O_2$ probes and their precursors were characterized by standard spectroscopic methods, and the data fully agreed with the proposed structures (Supporting Information, Figures S1−S12).

Table 1. Photophysical Data for the $^1O_2$ Probes

	λ_{abs} (nm, log ε)	λ_{ems} (nm)[b]	PLQY (%)[c]	τ_{obs} (ns)[d]	FI ratio[e]
DPBF	415 (4.26)	455	72 ± 7.4	1.46	turn-off
+ $^1O_2$[a]	298 (3.78)	nd[f]	nd[f]	nd[f]	
PPBF	411 (4.35)	476	6.4 ± 1.0	1.38	80
+ $^1O_2$[a]	324 (3.96)	370	0.78 ± 0.12	0.425	
PyPBF	438 (4.40)	512	28 ± 2.7	1.48	352
+ $^1O_2$[a]	358 (4.22)	398	6.1 ± 0.5	1.17	
StPBF	450 (4.50)	505	39 ± 6.0	2.29	14
+ $^1O_2$[a]	382 (4.16)	435	41 ± 8.2	1.58	

[a] O_2-saturated THF solutions containing 10 μM probe and 100 nM photosensitizer were photoirradiated under 365 nm for 100 s. [b] λ_{ex} = 415 nm (DPBF), 331 nm (PPBF), 358 nm (PyPBF), and 350 nm (StPBF). [c] Photoluminescence quantum yield relative to 9,10-diphenylanthracene (PLQY = 0.90, cyclohexane) as a standard. [d] Fluorescence lifetime determined through picosecond (λ_{ex} = 377 nm) time-correlated single photon counting techniques. [e] Fluorescence intensity (FI) ratio: PPBF, $FI_{370\ nm}/FI_{476\ nm}$; PyPBF, $FI_{398\ nm}/FI_{512\ nm}$; StPBF, $FI_{435\ nm}/FI_{505\ nm}$. [f] Not detected.

As expected, the $^1O_2$ probes exhibited significant red shifts in their fluorescence peak wavelengths relative to DPBF (10 μM in THF, $\Delta\nu = \nu_{ems}(DPBF) - \nu_{ems}(^1O_2\ probe)$: PPBF, 970 cm^{-1}; StPBF, 2180 cm^{-1}; PyPBF, 2450 cm^{-1})

due to the effective conjugation to the fluorophores. The probes are highly fluorescent with photoluminescence quantum yields (PLQYs) of 6.4−39%. To evaluate $^1O_2$ sensing properties, we employed a biscyclometalated Ir(III) complex, IrF (Scheme 1), as a $^1O_2$ photosensitizer because it has

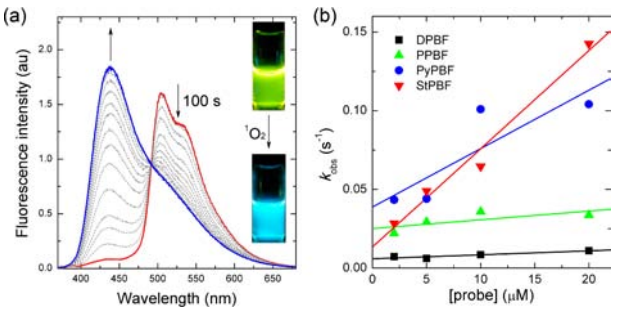

Figure 1. (a) Fluorescence response of 10 μM StPBF toward $^1O_2$. The arrows indicate the direction of the spectral changes. The inset photos show fluorescence emission of the StPBF solution before (top) and after (bottom) the $^1O_2$ generation. (b) Plots of observed reaction rates (k_{obs}) as a function of the concentration of the $^1O_2$ probes.

been proved to be highly efficient for $^1O_2$ generation.[29] As shown in Figure 1, 100 s photoirradiation (λ_{ex} = 365 nm) of an O_2-bubbled (30 min) THF solution containing 10 μM StPBF and 100 nM IrF led to fluorescence color changes from green to blue. The fluorescence peak wavelength shifted from 505 to 435 nm, and the corresponding fluorescence intensity (FI) ratio at 435 nm versus 505 nm (i.e., $FI_{435\ nm}/FI_{505\ nm}$) increased by a factor of 14. The clear isosbestic point at 490 nm indicates the absence of any fluorescent byproduct. By contrast, the ratiometric change was not observed without IrF or photoirradiation (Supporting Information, Figure S13a). In addition, the addition of an $^1O_2$ scavenger, 1 mM NaN_3,[30] abrogated the fluorescent $^1O_2$ response (Supporting Information, Figure S13b). These results unambiguously indicate that the fluorescence change was attributed to $^1O_2$. PPBF and PyPBF displayed similar fluorescence ratiometric responses to $^1O_2$ with changes in the fluorescence intensity ratios of factors of 80 (PPBF, $FI_{370\ nm}/FI_{476\ nm}$) and 352 (PyPBF, $FI_{398\ nm}/FI_{512\ nm}$), respectively (Table 1 and Supporting Information, Figure S14).

The UV−vis absorption spectra of 10 μM probes displayed hypsochromic shifts ($\Delta\nu = \nu_{abs}$(before reaction) − ν_{abs}(after reaction): StPBF, −3960 cm^{-1}; PyPBF, −5100 cm^{-1}; PPBF, −6530 cm^{-1}) upon the reaction with $^1O_2$, indicating products with wide band gap energies (Supporting Information, Figure S15). Positive mode ESI−MS spectra for the $^1O_2$ reaction product of PPBF revealed peaks at m/z = 409 and 425 mu (Supporting Information, Figure S16). These values correspond to [1,2-diketone + Na]$^+$ and [endoperoxide + Na]$^+$, respectively (see Scheme 1). It appeared that the dominant $^1O_2$ reaction product was 1,2-diketone because ^{13}C NMR spectra (100 MHz) for the product displayed two carbonyl peaks at δ 197.3 and 197.4 ppm (acetone-d_6; Supporting Information, Figure S17). HPLC chromatograms acquired during the $^1O_2$ reaction displayed the complete conversion of PPBF to a single product (Supporting Information, Figure S18). Indeed, the experimental UV−vis absorption spectrum of the product is in good agreement with a simulated spectrum of the 1,2-diketone of PPBF (TD-DFT, B3LYP/6-311+G(d,p)//uB3LYP/6-311+G(d,p):C-PCM (THF); Supporting Information, Figure S19 and Table S1). Taken together, the studies provide strong evidence that the probes react with $^1O_2$ to yield the 1,2-diketone having hypsochromically shifted fluorescence emission.

The observed rates (k_{obs}) for the reaction between $^1O_2$ and the probes were determined by monitoring the temporal changes in the fluorescence intensity ratios (StPBF, PyPBF, and PPBF) or the total fluorescence intensity (DPBF) during the continuous photoirradiation. The probe concentration was varied in the range of 2−20 μM to keep the pseudo first-order kinetics of the probe. As shown in Figure 1b, the plot of k_{obs} as a function of the probe concentration follows a linear line. The largest slope is observed for StPBF (6.25 M^{-1} s^{-1}), and the slope decreases in the order of PyPBF (3.71 M^{-1} s^{-1}) > PPBF (0.557 M^{-1} s^{-1}) > DPBF (0.252 M^{-1} s^{-1}). Although the slope cannot be equated with the reaction rate constant under the experimental conditions, the results reveal that the $^1O_2$ reactivity increases in proportion with the extent of π-conjugation. By contrast, the oxidation potentials of the probes displayed a weak correlation with the $^1O_2$ reactivity (Supporting Information, Figure S20).

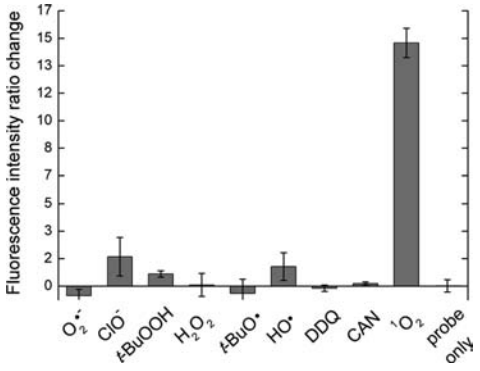

Figure 2. Fluorescence $^1O_2$ selectivity of StPBF over other reactive oxygen species ($O_2^{\bullet-}$, 1 mM KO_2; ClO^-, 1 mM NaOCl; 1 mM *t*-BuOOH; 1 mM H_2O_2; *t*-BuO$^\bullet$, 1 mM $FeSO_4$ + 100 μM *t*-BuOOH; $^\bullet$OH, 1 mM $FeSO_4$ + 100 μM H_2O_2) and chemical oxidants (CAN, 1 mM $(NH_4)_2Ce^{IV}(NO_3)_6$; DDQ, 1 mM 2,3-dichloro-5,6-dicyano-benzoquinone).

The $^1O_2$ probes exhibited great selectivity toward $^1O_2$ over other reactive oxygen species, including $O_2^{\bullet-}$, ClO^-,

(28) Kuninobu, Y.; Nishina, Y.; Nakagawa, C.; Takai, K. *J. Am. Chem. Soc.* **2006**, *128*, 12376–12377.

(29) You, Y.; Lee, S.; Kim, T.; Ohkubo, K.; Chae, W.-S.; Fukuzumi, S.; Jhon, G.-J.; Nam, W.; Lippard, S. J. *J. Am. Chem. Soc.* **2011**, *133*, 18328–18342.

(30) Harbour, J. R.; Issler, S. L. *J. Am. Chem. Soc.* **1982**, *104*, 903–905.

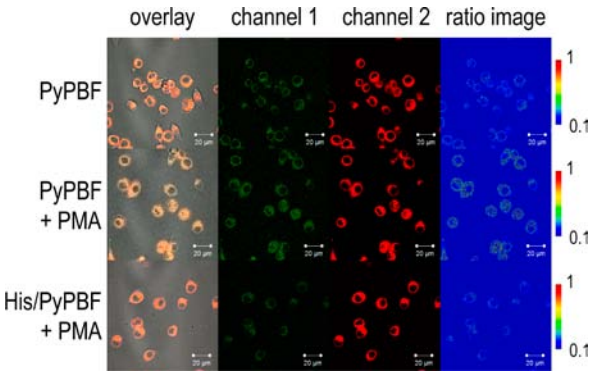

Figure 3. Fluorescent detection of intracellular $^1O_2$ in RAW 264.7 macrophage cells. Cells treated with 10 μM PyPBF for 30 min were visualized through dual channels: channel 1, λ_{ex} = 750 nm (two photon) and λ_{ems} = 377−481 nm; channel 2, λ_{ex} = 750 nm (two photon) and λ_{ems} = 490−568 nm; ratio image, channel 1/channel 2. The cells were subsequently incubated with 2 μM phorbol myristate acetate (PMA, 30 min) to stimulate endogenous $^1O_2$ generation (middle panels). Control experiments were performed for the cells preincubated with $^1O_2$ scavenger, 2 mM histidine (30 min; bottom panels).

t-BuO$^\bullet$, $^\bullet$OH, and H_2O_2, and chemical oxidants, such as $(NH_4)_2Ce^{IV}(NO_3)_6$ and DDQ (see Figure 2 for StPBF and Supporting Information, Figure S21 for other probes). Although the $^1O_2$ probes formed nano aggregates in aqueous solutions (pH 7.4, 50 mM HEPES + 0.1 M KCl + 10 vol % THF or CH_3CN) as observed in the FE−SEM image (Supporting Information, Figure S22), their fluorescent $^1O_2$ responses were retained (Supporting Information, Figure S23).

Having established the $^1O_2$ sensing capabilities of the probes, we performed two-photon fluorescence microscopic experiments to visualize endogenous $^1O_2$ in RAW 264.7 macrophage cells. We chose PyPBF because it exhibited the best cell permeability. PyPBF was nontoxic to the cells as judged from the bright-field images (Figure 3). RAW 264.7 cells treated with 10 μM PyPBF (30 min) produced intense fluorescence emission at λ_{ems} = 490−568 nm (channel 2) under two-photon excitation (λ_{ex} = 750 nm), whereas the fluorescence emission due to the 1,2-diketone of PyPBF at λ_{ems} = 377−481 nm (channel 1) was barely detected (Figure 3). Subsequent stimulation of the cells by 2 μM phorbol myristate acetate (PMA)[31] provoked a fluorescence increase in channel 1, indicating endogenous production of $^1O_2$. The corresponding increases in the fluorescence intensity ratios of the channel 1 images over the channel 2 images were greater than the standard deviations (Supporting Information, Figure S24). Additional micrographs are included in Supporting Information, Figure S25. As expected for the $^1O_2$ probe, pretreatment with 2 mM histidine, an intracellular $^1O_2$ scavenger,[32] suppressed the 1,2-diketone fluorescence. To the best of our knowledge, this is the first visualization of intracellular $^1O_2$ by ratiometric fluorescent signaling.

To summarize, we developed a series of ratiometric fluorescent probes for the detection of $^1O_2$. The probes underwent an irreversible reaction with $^1O_2$, producing hypsochromically shifted fluorescence. The ratiometric responses were not affected by the probe concentrations (Supporting Information, Figure S26), demonstrating the benefit of the ratiometric fluorescent signaling. The probes were capable of detecting $^1O_2$ among various reactive oxygen species. We further established that greater $^1O_2$ sensitivity could be accomplished using the isobenzofuran platforms with elongated π-conjugation. Finally, biological utility was demonstrated by dual channel two-photon fluorescent visualization of endogenous $^1O_2$ in macrophage cells.

Acknowledgment. This work was supported by the CRI (W.N.), GRL (2010-00353) (W.N.), and WCU (R31-2008-000-10010-0) (W.N.) programs from the National Research Foundation (NRF) of Korea.

Supporting Information Available. Experimental details; scheme depicting synthetic routes to PPBF and PyPBF; figures displaying copies of ^1H and ^{13}C NMR spectra of the $^1O_2$ probes and their precursor, fluorescence spectra obtained without IrF nor photoirradiation, or in the presence of NaN_3, fluorescence $^1O_2$ responses of PPBF and PyPBF, UV−vis absorption changes of the $^1O_2$ probes, the ESI−MS spectra, ^{13}C NMR spectrum of the reaction product of PPBF, HPLC chromatograms, TD−DFT calculation results, cyclic voltammograms, $^1O_2$ selectivity of PPBF and PyPBF, the FE−SEM image of the aggregates of PyPBF, fluorescent $^1O_2$ responses and selectivity of PyPBF in buffer solution, calculated fluorescence intensity ratios for the fluorescence micrographs, more cell images, and the fluorescent $^1O_2$ responses of StPBF at different probe concentrations; tables listing the summary of TD−DFT calculation results and the Cartesian coordinates of the optimized geometries. This material is available free of charge via the Internet at http://pubs.acs.org.

(31) Kanofsky, J. R.; Hoogland, H.; Wever, R.; Weiss, S. J. *J. Biol. Chem.* **1988**, *263*, 9692–9696.
(32) Tomita, M.; Irie, M.; Ukita, T. *Biochemistry* **1969**, *8*, 5149–5160.

The authors declare no competing financial interest.